Molecular engineering for optical properties of 5-substituted-1,10-phenanthroline-based Ru(II) complexes

Elodie Rousset, Olivier Mongin, Juliette Moreau, Latevi Max Lawson Daku, Marc Beley, Philippe Gros, Sylviane Chevreux, Mireille Blanchard-Desce, Gilles Lemercier

▶ **To cite this version:**

Elodie Rousset, Olivier Mongin, Juliette Moreau, Latevi Max Lawson Daku, Marc Beley, et al.. Molecular engineering for optical properties of 5-substituted-1,10-phenanthroline-based Ru(II) complexes. Dalton Transactions, 2021, 50 (29), pp.10119-10132. 10.1039/D1DT00886B . hal-03251344

HAL Id: hal-03251344
https://hal.science/hal-03251344v1

Submitted on 1 Oct 2021

HAL is a multi-disciplinary open access archive for the deposit and dissemination of scientific research documents, whether they are published or not. The documents may come from teaching and research institutions in France or abroad, or from public or private research centers.

L'archive ouverte pluridisciplinaire **HAL**, est destinée au dépôt et à la diffusion de documents scientifiques de niveau recherche, publiés ou non, émanant des établissements d'enseignement et de recherche français ou étrangers, des laboratoires publics ou privés.

Molecular engineering for optical properties of 5-substituted-1,10-phenanthroline-based Ru(II) complexes

Elodie ROUSSET,[a] Olivier MONGIN,[b] Juliette MOREAU,[a] Latévi Max LAWSON-DAKU[c], Marc BELEY,[d] Philippe C. GROS,[d] Sylviane CHEVREUX,[a,e] Mireille BLANCHARD-DESCE,[f] Gilles LEMERCIER[a *]

[a] Université de Reims Champagne-Ardenne, ICMR UMR CNRS n° 7312 BP 1039 – 51687 Reims cedex 2, France – gilles.lemercier@univ-reims.fr; [b] Univ Rennes, CNRS, ISCR (Institut des Sciences Chimiques de Rennes) – UMR 6226, F-35000 Rennes, France [c] Dépt. de Chimie Physique, Université de Genève, 30, quai E. Ansermet, Geneva 4, CH-1211, Switzerland; [d] Université de Lorraine, CNRS, L2CM, Nancy, F54000, France; [e] Chimie ParisTech, PSL University, CNRS, Institut de Recherche de Chimie Paris, 75005 Paris, France; [f] Université Bordeaux, ISM, Centre National de la Recherche Scientifique, UMR 5255, F-33400 Talence, France.

Abstract

A series of homo- and heteroleptic Ru(II) complexes **$[Ru(phen)_{3-n}(phen\text{-}X)_n](PF_6)_2$** (n=0-3, X = CN, epoxy, H, NH_2) were prepared and characterized. The influence of electron-withdrawing or electron-releasing substituents of the 1,10-phenanthroline ligands on the photo-physical properties was evaluated. It reveals fundamental interests in the fine tuning of redox potentials and photo-physical characteristics, depending both on the nature of the substitution of the ligand, and on the symmetry of the related homo- or heteroleptic complex. These complexes exhibit linear absorption and two-photon absorption (2PA) cross-sections over a broad range of wavelength (700-900 nm) due to absorption in the intra-ligand charge transfer (ILCT) and the metal-to-ligand charge transfer (MLCT) bands. These 2PA properties were more particularly investigated in the 700-1000 spectral range for a family of complexes bearing electro-donating ligands (phen-NH_2).

Introduction

For the past decades, Ruthenium(II) polypyridyl complexes attracted a considerable interest for the peculiar linear and nonlinear optical (NLO) properties associated with their triplet metal-to-ligand charge transfer (^{3}MLCT) excited state,[1] as they usually present long luminescence lifetime in the range of few microseconds.[2] Advantage can be taken of their excited-state re-absorption for optical power limiting (OPL) applications,[3] as well as the energy and the triplet character of the MLCT excited-state, in their use as oxygen sensors[4] or photosensitizers.[5] Ru(II)-polypyridyl complexes have also been intensively studied due to their stability, inertness, and synthetic tailorability.[6] The achievable controlled elaboration of either homo- and heteroleptic complexes leads to different symmetries and, involving electro-withdrawing and/or –donating

functionalized ligands, allows the fine-tuning of their electronic and optical properties. Comprehensive understanding of the effect of functionalization of molecular entities or the imposed symmetry on the linear and nonlinear optical (NLO) properties is therefore of major interest.

This has prompted several recent theoretical and experimental studies concerning organic as well as organometallic systems. In this domain, several structural parameters have been reported to deeply influence this potential coherent electronic coupling[7] such as the nature of the branches and the core, as well as node, and peripheral moieties. Blanchard-Desce *et al*. have shown that branched systems based on dipolar chromophores connected *via* a functionalised triphenylamine core give rise to a sizeable electronic coupling between branches and specific optical properties.[8] A metal may not only act as either a strong electron donor or acceptor but also as a template for the symmetric (or asymmetric) arrangement of ligands, a molecular engineering relatively difficult to achieve with pure organic compounds. For example, previous studies showed that coordination chemistry is a very useful tool for the design of either tetrahedral or octahedral octupolar NLO-phores. The molecular quadratic hyperpolarizability (β) values may be strongly influenced by the symmetry of the complexes, the nature of the ligands, the nature of the metallic centres[9] and their oxidation states.[10]

Owing to its wide-range of applications[11] (photodynamic therapy or PDT,[12] confocal microscopy,[13] micro-fabrication of objects[14] and optical power limiting, OPL[15]), the two-photon absorption process (2PA), consisting in the simultaneous absorption of two photons, is a very attractive third order nonlinear optics effect. A number of factors influence the 2PA magnitude, among them electron delocalization and intra-molecular charge transfer (ICT) phenomena play an important role.[16] In this field, coordination complexes, and especially Ru(II) edifices[17,3d] have undisputable advantages. A few organometallic ruthenium complexes, and related dendritic structure[18] were studied for their nonlinear response,[19,20,17b] and their OPL efficiency.[3a-c] Two-photon absorption properties of octupolar coordination Ru(II) complexes were also investigated. Quarter-pyridinium ligand led to moderate 2PA efficiency (up to 180 GM[21] at 750 nm)[22] while a more conjugated ligand based on a diamino-styryl bipyridine afforded higher 2PA cross-section values[23] (σ_{2PA} up to 2200 GM between 765 nm and 965 nm – keeping in mind that 2PA cross-sections values may depend on the technique used and especially Z-Scan measurements compared to the two-photon excited luminescence technique, "2PEF"). M. Humphrey *and coll*. published the second and third order optical properties (determined by using hyper-Rayleigh scattering –HRS-, and Z-Scan measurements, respectively) of D_3 symmetric octupolar alkynylruthenium edifices, and compared them to the NLO properties of the linear analogues.[24]

We report here the study of the influence of electron-withdrawing and electron-donating substituents (R) in the 5-position (or 5,6-position concerning epoxide derivative) of the 1,10-phenanthroline ligand (**phen-X**) on linear and nonlinear (two-photon absorption) properties of related Ru(II) complexes. We also explored the influence of the core symmetry of the complexes by the synthesis and the characterization of hetero- and homoleptic complexes (see Figure 1). Three series of ruthenium(II) complexes bearing substituted **phen-X** ligands, where X = -H, CN, epoxy or NH_2 are presented. These complexes exhibit linear absorption and quite large 2PA cross-sections over a broad wavelength range (700-900 nm) due to absorption in the intra-ligand charge transfer (ILCT) bands as well as in the metal-to-ligand charge transfer (MLCT) electronic transitions.

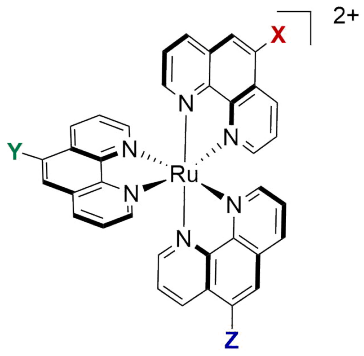

Figure 1. Homoleptic (X=Y=Z) and heteroleptic Ru(II) complexes, where X, Y, and Z correspond to electron-withdrawing or electron-donating substituents; PF_6^- was used as counterion.

Results and discussion

Synthesis. The three functionalized 1,10-phenanthroline ligands **phen-X** involved in the complexation of a Ru(II) metallic centre were synthesized from the commercially available 1,10-phenanthroline (**phen)**, according to two synthetic pathways already described in the literature and presented in Scheme 1. On one hand, 5-nitro-1,10-phenanthroline (**phen-NO_2**) was synthesized in concentrated acidic medium, before being reduced by hydrazine hydrate to obtain the 5-amino-1,10-phenanthroline derivative (**phen-NH_2**).[25] On the other hand, the oxidation of **phen** by commercial bleach leading to 5,6-epoxide-5,6-dihydro-,10-phenanthroline (**phen-epox**) was followed by a cyanation to obtain the desired 5-cyano-1,10-phenanthroline compound (**phen-CN**).[26]

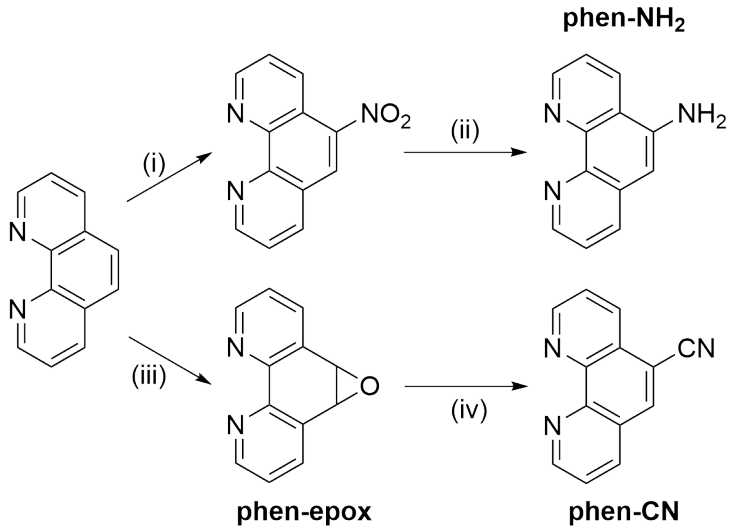

Scheme 1. Ligands synthesis, reagents and conditions: (*i*) H_2SO_4, HNO_3, reflux, 3h (yield = 90%) ; (*ii*) NH_2-NH_2.H_2O, Pd/C, EtOH, reflux overnight (yield = 60%) ; (*iii*) commercial bleach, NBu_4^+, HSO_4^-, pH=8.6, r.t., 1 h (yield = 35%) ; (*iv*) KCN 1M, r.t., overnight (yield = 55%).

The **phen-CN** and **phen-NH_2** ligands were involved in the synthesis of their corresponding Ru(II) homoleptic complexes. The preparation involving three equivalents of **phen-X** ligand with one equivalent of **[Ru(dmso)$_4$Cl$_2$]** as Ru(II) precursor derivative is presented in Scheme 2.

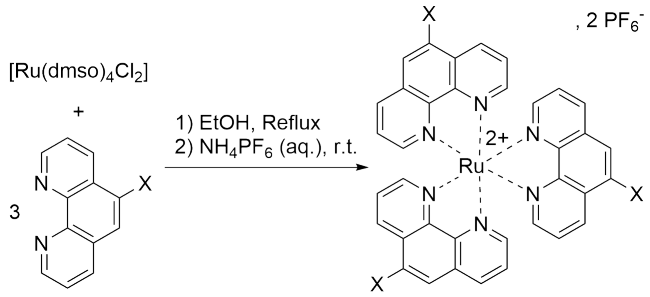

Scheme 2. Synthesis and molecular structure of the homoleptic complexes, X = CN (yield = 40%) and X=NH_2 (yield = 55%).

In order to allow the fine-tuning of the optical properties, two series of heteroleptic complexes **[Ru(phen)$_2$(phen-X)](PF$_6$)$_2$** (where X = CN[26c], NH_2 at the 5th position of the phen,[25] or the 5,6-epoxy analogue) and **[Ru(phen)(phen-X)$_2$](PF$_6$)$_2$** (where X = NH_2) were synthetized. For the first mentioned series, the desired **phen-X** ligand was involved with the previously synthesized precursor complex **[Ru(phen)$_2$Cl$_2$]**[27] (Scheme 3) to form a **[Ru(phen)$_2$(phen-X)](PF$_6$)$_2$** series.

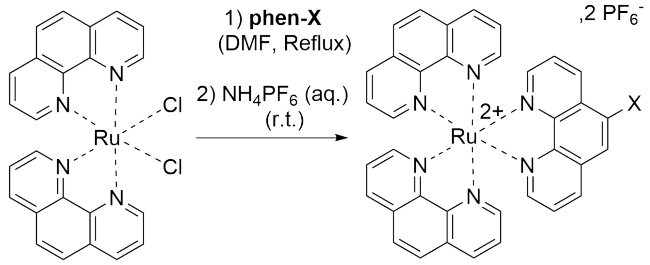

Scheme 3. Synthesis of the heteroleptic complexes **[Ru(phen)$_2$(phen-X)](PF$_6$)$_2$**, where X = CN,[26c] epoxide and NH_2[25] (yield = 85%, 32% and 89%, respectively).

The synthesis of the other series of heteroleptic complex is usually presented as more difficult as it requires the formation of the **[Ru(phen-X)$_2$Cl$_2$]** precursor from non-commercial (and therefore of higher added value) ligands.[28] The key of the simplified procedure reported herein resides in the non-isolation of this precursor after reaction of **[Ru(dmso)$_4$Cl$_2$]**[29] with two equivalents of **phen-X** ligand: the ethanolic solution was heated overnight at reflux followed by the direct addition of one equivalent of **phen** ligand at room temperature. The reaction mixture was then heated at reflux overnight, leading the desired **[Ru(phen)(phen-X)$_2$](PF$_6$)$_2$** series (where X = NH_2) (Scheme 4). It has to be pointed out that this synthesis could also be performed inspired by another published procedure for the preparation of mixed complexes of Ru(II) with 2,2'-dipyridyl.[30] All ligands and complexes were characterized by ^{1}H (and ^{13}C when possible) nuclear magnetic resonance (NMR), infrared (IR) spectroscopies and elemental analysis (see experimental section). As previously published by us, and others, all the following studies were performed on the potential mixtures of diastereoisomers (see ^{1}H NMR spectra, Figures S1 to S7 of the supplementary material). As illustrated by the reported lifetimes (and related mono-exponential fits – see ESI Fig. S19-S23), this has no significant influence on our results and the analysis of the observed trends in "molecular structure – properties" correlations between families of complexes and within each family. Furthermore, the electronic excitations calculations performed on the *fac*- and *mer*-[Ru(phen-

$NH_2)_3]^{2+}$ stereoisomers show that both stereoisomers have very similar frontiers molecular orbitals and nearly identical absorption spectra.

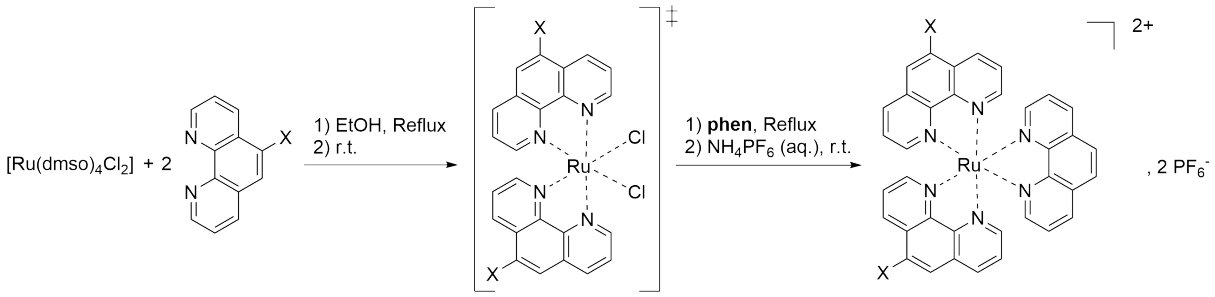

Scheme 4. Synthesis of heteroleptic complexes **$[Ru(phen)(phen\text{-}X)_2](PF_6)_2$** X = NH_2 (Yield = 30%)

Electrochemical measurements.

The electrochemical properties of the series of complexes (**$[Ru(phen)_3]^{2+}$**, **$[Ru(phen)_2(phen\text{-}CN)]^{2+}$**, **$[Ru(phen\text{-}CN)_3]^{2+}$**, **$[Ru(phen)_2(phen\text{-}epox)]^{2+}$**, **$[Ru(phen)_2(phen\text{-}NH_2)]^{2+}$** and **$[Ru(phen\text{-}NH_2)_3]^{2+}$**) were measured in acetonitrile using $TBAPF_6$ as the supporting electrolyte and the corresponding voltammograms can be found in ESI (Figure S8 to S13). Results are summarized in Table 1 along with the band gap, defined as the difference between the first reduction and oxidation peaks and to be correlated with the HOMO-LUMO energy gap.

The results obtained in acetonitrile confirm that the nature of the ligand around the Ru(II) cation plays a crucial role in the electrochemical behaviour of the homoleptic and heteroleptic complexes. For the compounds designed with an electron withdrawing substitution of the 1,10-phenanthroline ligand (X = CN), each cyclo-voltammogram present a reversible mono-electronic process, classically attributed to the oxidation of the metal centre from Ru(II) to Ru(III).[31,32] The oxidation peaks appear at 1.34 and 1.40 V *vs.* SCE for **$[Ru(phen)_2(phen\text{-}CN)]^{2+}$** and **$[Ru(phen\text{-}CN)_3]^{2+}$**, respectively.

Table 1. Electrochemical properties of the Ru(II) complexes synthetized; Potentials measured at 25°C and quoted in volts (V) *vs* SCE. Under these conditions $E_{1/2\,(Fc+/Fc)} = 0.39$ V.

Complexes	$E_{1/2}$ (V) Ru(III)/Ru(II) (ΔE_p / mV)	$E_{1/2}$ (V) L/L^- (ΔE_p / mV)	ΔE/ eV
$[Ru(phen)_3]^{2+}$ [32]	1.27	-1.35	2.63
	(90)	(85)	
$[Ru(phen)_2(phen\text{-}CN)]^{2+}$	1.34	-1.08	2.42
	(90)	(100)	
$[Ru(phen\text{-}CN)_3]^{2+}$	1.40	-1.10	2.50
	(100)	(80)	
$[Ru(phen)_2(phen\text{-}epox)]^{2+}$	1.30	-1.13	
	(110)	(irr.)	
$[Ru(phen)_2(phen\text{-}NH_2)]^{2+}$	1.35	-1.38	2.73
	(90)	(85)	
$[Ru(phen\text{-}NH_2)_3]^{2+}$	1.46	-1.44	2.90
	(40)	(80)	

Compared to the archetypal homoleptic **[Ru(phen)$_3$]$^{2+}$** complex, for which the oxidation potential is reported at 1.27 V *vs.* SCE,[32,33] the addition of nitrile substituents yields to complexes harder to oxidise. This result is *a priori* in accordance with the Hammett parameter of a cyano group[34] in conjunction with the increased number of substituted phenanthroline ligands across this series. A similar effect is observed for the other electron withdrawing epoxide group with the oxidation potential increasing from 1.28 for **[Ru(phen)$_3$]$^{2+}$** to 1.30 V *vs.* SCE for **[Ru(phen)$_2$(phen-epox)]$^{2+}$**. On the negative part, voltammograms present a monoelectronic process at -1.08 and -1.10 V *vs.* SCE for **[Ru(phen)$_2$(phen-CN)]$^{2+}$** and **[Ru(phen-CN)$_3$]$^{2+}$**, respectively.

Such processes are classically attributed to the reduction of the ligand(s).[35] Although the previously described reduction peaks were qualified of reversible, the reduction peak of **[Ru(phen)$_2$(phen-epox)]$^{2+}$** appears to be irreversible at -1.13 V *vs.* SCE, showing that the electron is injected into the (phen-epox) where an irreversible reduction of the epoxide group is induced.

Although the case of the electron withdrawing substitution appears to follow what is usually observed in the (electro-)chemistry of divalent ruthenium polypyridyl complexes, the study of electron donating NH_2 substituents reveals a less classical behaviour. On the oxidation side, two anodic peaks are observed for each compound containing phen-NH_2 ligands. A first irreversible process appears at 1.26 and 1.20 V *vs.* SCE for **[Ru(phen)$_2$(phen-NH$_2$)]$^{2+}$** and **[Ru(phen-NH$_2$)$_3$]$^{2+}$** respectively and is tentatively attributed to the oxidation of the amine-containing ligand. The oxidation of the ruthenium centre seems to occur at higher potential (1.35 and 1.46 *vs* SCE for **[Ru(phen)$_2$(phen-NH$_2$)]$^{2+}$** and **[Ru(phen-NH$_2$)$_3$]$^{2+}$**, respectively). This intricate and quite complex phenomena of oxidation potentials of Ru(II) coalescing with the one of the amine group was previously described by T. J. Meyer and co-workers.[36] Polypyridyl complexes of ruthenium containing aromatic amine groups as 5-amino-1,10-phenanthroline undergo oxidative electro-polymerization reactions. For **[Ru(phen-NH$_2$)$_3$]$^{2+}$**, repeated cycling on a Pt wire at 100 mV/s between 0.8 V and 1.7 V *vs.* SCE, produced a fast current increase of the Ru(II)/Ru(III) wave with scan numbers signing an electro-activity enhancement, which can be attributed to a polymer growth at the electrode surface (Figure 2a, top).[36,37]

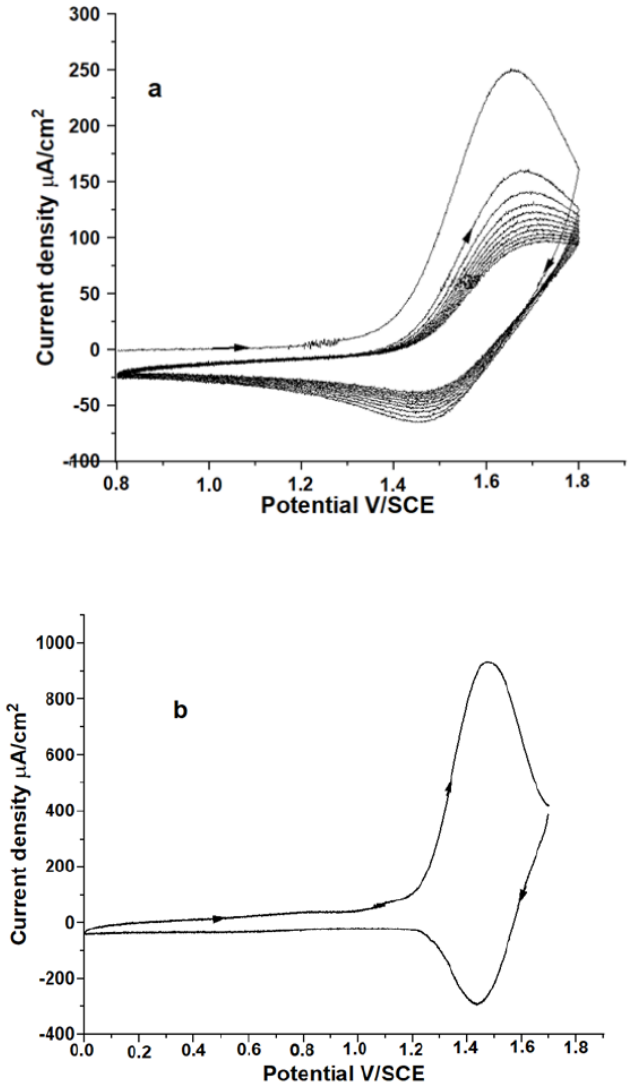

Figure 2. **a** *top*: Repeated cyclic voltammograms from 0.8 to 1.7 V *vs.* SCE of $\mathbf{[Ru(phen\text{-}NH_2)_3]^{2+}}$ in CH_3CN/0.1M Bu_4NPF_6 on platinum electrode; **b** *bottom*: Cyclic voltammogram of the platinum electrode coated with the film poly-$\mathbf{[Ru(phen\text{-}NH_2)_3]^{2+}}$ in fresh electrolyte solution.

After 10 scans, the yellow film on the electrode was extensively washed with acetonitrile, acetone and dimethylformamide to be characterized by cyclic voltammetry between 0 V and 1.7 V *vs.* SCE in monomer-free electrolyte (Figure 2b, bottom). The small separation between oxidative and reductive waves ΔE_p < 40 mV characterizes the immobilised Ru(III)/Ru(II) couple in the film. On the negative side, the first potential at -1.38 V can be assigned to reduction of the ligand **phen** in the $\mathbf{[Ru(phen)_2(phen\text{-}NH_2)]^{2+}}$ species**,** while for $\mathbf{[Ru(phen\text{-}NH_2)_3]^{2+}}$ the first reduction potential at -1.44 V corresponds to the reduction of the ligand **phen-NH$_2$**.

To corroborate the attribution of the electronic processes, the HOMO and LUMO levels of the homoleptic $[Ru(L)_3]^{2+}$ (L = phen, phen-NH_2, phen-CN) and heteroleptic $\mathbf{[Ru(phen)_2(L)]^{2+}}$ (L = phen-NH_2, phen-CN) complexes have been characterized within DFT[38] from calculations performed with the statistical average of orbital potentials (SAOP)[39] exchange-correlation potential and the all-electron TZ2P Slater-type (STO) basis set of triple-ζ doubly polarized quality[40] (see the Computational details section). These frontier levels are

represented in Figure 3. For **[Ru(phen)$_3$]$^{2+}$**, **[Ru(phen)$_2$(phen-CN)]$^{2+}$** and **[Ru(phen-CN)$_3$]$^{2+}$**, the HOMOs are metal-centred while the LUMOs are ligand-centred π^* orbitals.

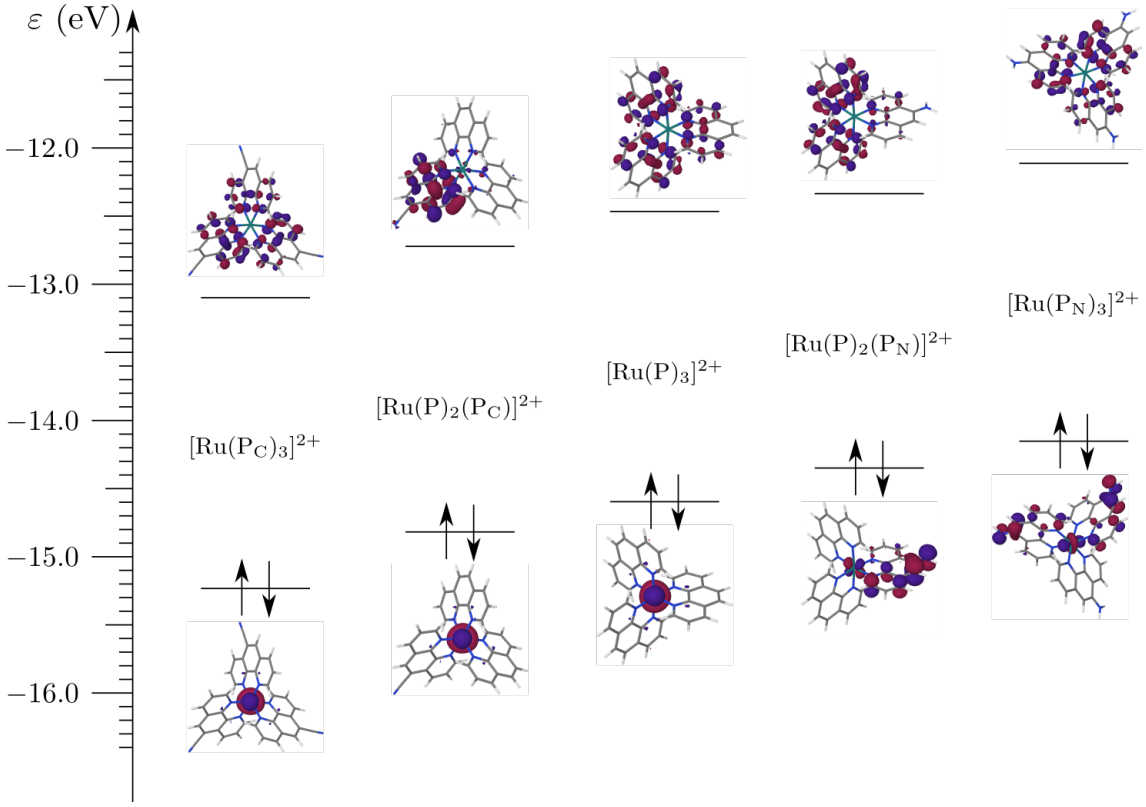

Figure 3. Calculated HOMO and LUMO levels of the homoleptic [Ru(L)$_3$]$^{2+}$ (L = P, P$_C$, P$_N$) and heteroleptic [Ru(P)$_2$(L)]$^{2+}$ (L = P, P$_C$, P$_N$) complexes (P = phen, P$_C$ = phen-CN, P$_N$ = phen-NH$_2$; iso-surfaces calculated for isovalues of ±0.04 au; SAOP/TZ2P results).

The LUMO of [Ru(phen)$_3$]$^{2+}$ is found to be delocalized over the three ligands; likewise for **[Ru(phen-CN)$_3$]$^{2+}$** the delocalization is over the phen moieties of the three ligands. This can be easily related to the fact that the first reduction wave occurs on the π-accepting 1,10-phenanthroline ligand meaning that the LUMO is localized on this moiety. It also follows that the oxidation of **[Ru(phen)$_3$]$^{2+}$**, **[Ru(phen)$_2$(phen-CN)]$^{2+}$** and **[Ru(phen-CN)$_3$]$^{2+}$** can be identified as the oxidation of the metal centre from Ru(II) to Ru(III) and that their first reduction potential corresponds to the one of the ligands. For **[Ru(phen)$_2$(phen-NH$_2$)]$^{2+}$** (resp., **[Ru(phen-NH$_2$)$_3$]$^{2+}$**), the HOMO is mainly centred on the phen-NH$_2$ ligands (respectively two of the phen-NH$_2$ (or P$_N$) ligands) and exhibits a small metallic contribution; the ligand contributions correspond to a π orbital involving the lone pair of the -NH$_2$ group and with a nodal plane between the C-NH$_2$ bond. The LUMO of **[Ru(phen)$_2$(phen-NH$_2$)]$^{2+}$** is a π^* orbital delocalized mainly over the phen ligands and the LUMO of [Ru(phen-NH$_2$)$_3$]$^{2+}$ is a π^* orbital delocalized over the phen moieties of the three ligands. For **[Ru(phen)$_2$(phen-NH$_2$)]$^{2+}$** and **[Ru(phen-NH$_2$)$_3$]$^{2+}$**, these results support the attribution of their observed first oxidation processes to the oxidation of the amine-containing ligand. They also corroborate the identification of the reduction process observed for **[Ru(phen)$_2$(phen-NH$_2$)]$^{2+}$** and **[Ru(phen-NH$_2$)$_3$]$^{2+}$** to the reduction of the 1,10-phenanthroline ligand and the phen-NH$_2$ ligand, respectively.

Taking the unsubstituted [Ru(phen)$_3$]$^{2+}$ complex as reference, one notes in Figure 3 that the energies of the HOMO (ε_{HOMO}) and LUMO (ε_{LUMO}) decrease with the number of electron-withdrawing CN substituents and that

these energies increase with the number of electron-donating NH_2 groups. The values found for ε_{HOMO} and ε_{LUMO} are summarized in Table 2, with the corresponding HOMO-LUMO energy differences $\Delta\varepsilon_{HL}$. For **[Ru(phen)$_3$]$^{2+}$**, **[Ru(phen)$_2$(phen-CN)]$^{2+}$** and **[Ru(phen-CN)$_3$]$^{2+}$**, the predicted $\Delta\varepsilon_{HL}$ values are ~0.5 eV smaller than those observed in the electrochemistry measurements (Table 1):

Table 2. Calculated energies of the HOMO (ε_{HOMO}) and LUMO (ε_{LUMO}) levels in **[Ru(phen-CN)$_3$]$^{2+}$**, **[Ru(phen)$_2$(phen-CN)]$^{2+}$**, **[Ru(phen)$_3$]$^{2+}$**, **[Ru(phen)$_2$(phen-NH$_2$)]$^{2+}$** and **[Ru(phen-NH$_2$)$_3$]$^{2+}$** and associated HOMO-LUMO energy differences $\Delta\varepsilon_{HL}$ (SAOP/TZ2P results)

	ε_{HOMO} (eV)	ε_{LUMO} (eV)	$\Delta\varepsilon_{HL}$ (eV)
[Ru(phen-NH$_2$)$_3$]$^{2+}$	-14.147	-12.108	2.039
[Ru(phen)$_2$(phen-NH$_2$)]$^{2+}$	-14.344	-12.330	2.014
[Ru(phen)$_3$]$^{2+}$	-14.591	-12.461	2.130
[Ru(phen)$_2$(phen-CN)]$^{2+}$	-14.813	-12.717	2.096
[Ru(phen-CN)$_3$]$^{2+}$	-15.228	-13.094	2.134

For **[Ru(phen)$_2$(phen-NH$_2$)]$^{2+}$** and **[Ru(phen-NH$_2$)$_3$]$^{2+}$**, gaps reported in Table 1 involve the Ru(II)/Ru(III) oxidation process. Appropriate comparison considers the gaps obtained from their first irreversible oxidation processes occurring at 1.26 and 1.20 V *vs*. SCE for **[Ru(phen)$_2$(phen-NH$_2$)]$^{2+}$** and **[Ru(phen-NH$_2$)$_3$]$^{2+}$**, respectively: in both cases, the gaps corresponds to 2.64 eV, a value ~0.5 eV larger than the predicted $\Delta\varepsilon_{HL}$ values (Table 2). This ~0.5 eV systematic underestimation of the experimental gaps can be ascribed to (*i*) the neglect of solvent effects in our calculations performed in the gas phase and (*ii*) the fact that the observed redox processes involved structural reorganization of the complexes and the solvent which cannot be accounted for by the present calculations.

In Figure 4, the first oxidation and reduction potentials of the complexes are plotted as functions of the calculated values of ε_{HOMO} and ε_{LUMO}, respectively. An excellent linear correlation is observed between the first oxidation potential and ε_{HOMO} ($R^2 = 0.977$):

$$E_{1/2}\,[\text{V vs. SCE}] = -0.18 \times \varepsilon_{HOMO}\,[\text{eV}] - 1.34\,[\text{V } \textit{vs.}\ \text{SCE}] \quad (1)$$

Similarly, a satisfactory linear correlation is observed between the first reduction potential and ε_{LUMO} ($R^2 = 0.817$):

$$E_{1/2}\,[\text{V vs. SCE}] = -0.40 \times \varepsilon_{LUMO}\,[\text{eV}] - 6.32\,[\text{V } \textit{vs.}\ \text{SCE}] \quad (2)$$

The observed linear correlations validate the present analysis of the results of the electrochemistry experiments based on gas-phase DFT calculations with the SAOP exchange-correlation potential. Furthermore equations (1) and (2) prove appealing for the prediction of the first oxidation and reduction potentials of Ru(II) complexes of phen and its derivative ligands.

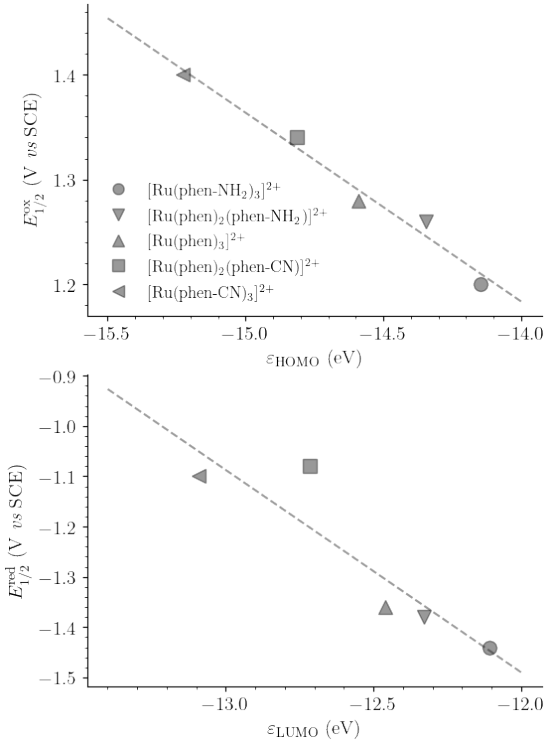

Figure 4. Plots of the first oxidation and reduction potentials of **[Ru(phen-CN)$_3$]$^{2+}$**, **[Ru(phen)$_2$(phen-CN)]$^{2+}$**, **[Ru(phen)$_3$]$^{2+}$**, **[Ru(phen)$_2$(phen-NH$_2$)]$^{2+}$** and **[Ru(phen-NH$_2$)$_3$]$^{2+}$** as functions of their calculated HOMO and LUMO energies, respectively. The dashed lines correspond to the results of linear least-square regression calculations

Absorption spectroscopy. The absorption spectra of all the complexes were measured in acetonitrile and are presented Figure 5 while maximum wavelength and extinction coefficients are summarized in Table 3. All compounds present similar features, characteristic of ruthenium polypyridyl complexes: (*i*) a very intense band between 250 and 280 nm (λ_{max} = 264 nm in **[Ru(phen)$_3$](PF$_6$)$_2$**, which can be attributed to intra-ligand (IL) transitions ($\pi_L \rightarrow \pi_L^*$), (*ii*) a broad band around 450 nm assigned to $d_{Ru(II)} \rightarrow \pi^*_{phen}$ metal-to-ligand charge-transfer (^{1}MLCT) transitions (see Table 3), which is characteristic of ruthenium(II) complexes involving polypyridyl type ligands,[41,1] (*iii*) for X = NH$_2$, a broad band between 300 and 400 nm, transition which may be attributed to an intra-ligand charge-transfer (ILCT) transition involving a charge flow from the NH$_2$ electro-releasing substituent to the 1,10-phenanthroline moiety. The band attributions are supported by the results of TDDFT calculations performed in the gas phase using the statistical average of orbital potentials (SAOP) exchange-correlation potential (for additional information, see the "Computational details" paragraph). For **[Ru(phen)$_3$]$^{2+}$**, the band centred at about 450 nm could be assigned to three intense MLCT transitions predicted at 458, 464 and 466 nm (see Table S1, transitions $S_0 \rightarrow S_n$ with n = 13, 15, 17). The corresponding MLCT transitions in **[Ru(phen-NH$_2$)$_3$]$^{2+}$** are predicted to be more numerous and slightly blue-shifted, taking place in the 435-462 nm range (see Table S3, transitions $S_0 \rightarrow S_n$ with n = 25, 26, 28, 29, 32). As for these intense MLCT transitions in **[Ru(phen-CN)$_3$]$^{2+}$**, they are found to be red-shifted, occurring at 469, 472 and 492 nm (see Table S5, transitions $S_0 \rightarrow S_n$ with n = 15-17).

For **[Ru(phen)$_3$]$^{2+}$** and **[Ru(phen-CN)$_3$]$^{2+}$**, the low-energy part of the visible band is also due to MLCT transitions of weaker to vanishing intensities (see Tables S1 and S3 in the ESI). This is also the case for **[Ru(phen-NH$_2$)$_3$]$^{2+}$**, albeit a certain inter- and intra-ligand charge transfer character due to transitions of weak to

vanishing intensities coupled with a small MLCT character (see Table S5). For the **[Ru(phen-NH$_2$)$_3$]$^{2+}$** complex, the intense intra-ligand charge transfer (ILCT) transitions involving a NH_2 → phen charge flow have been identified and were found to take place at 416-418 nm (see Table S3, transitions $S_0 \rightarrow S_n$ with n = 33-36): this is in good agreement with experiments, the ILCT absorption band being experimentally observed at *ca* 370 nm. The small discrepancy between theory and experiment can be ascribed to the choice of the approximate exchange-correlation potential and to the neglect in our gas-phase calculations of solvation effects, which may include specific interactions like H-bond between phen-NH_2 ligands and the acetonitrile solvent. In all cases, the large width of this absorption band can be mainly ascribed to vibronic broadenings and/or the overlap of more bands corresponding to different close-lying electronic transitions.

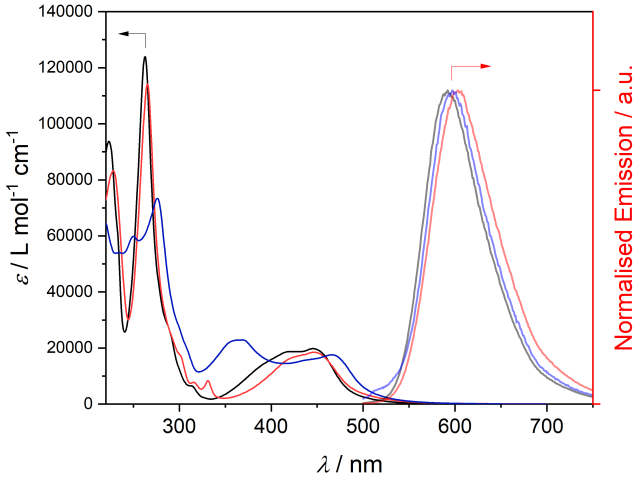

Figure 5. Absorption in molar extinction coefficient and normalised luminescence spectra at room temperature (λ_{exc} = 450 nm), in acetonitrile of homoleptic complexes **[Ru(phen)$_3$](PF$_6$)$_2$** (black/grey), **[Ru(phen-CN)$_3$](PF$_6$)$_2$** (blue/light blue), and **[Ru(phen-NH$_2$)$_3$](PF$_6$)$_2$** (red/light red).

In summary, homoleptic complexes bearing electro-withdrawing and electro-donating groups ((**[Ru(phen-CN)$_3$](PF$_6$)$_2$**) and **[Ru(phen-NH$_2$)$_3$](PF$_6$)$_2$**), respectively), were compared to the **[Ru(phen)$_3$](PF$_6$)$_2$** parent complex. The absorption spectrum of **[Ru(phen-CN)$_3$](PF$_6$)$_2$** is very similar to that of **[Ru(phen)$_3$](PF$_6$)$_2$**, whereas for **[Ru(phen-NH$_2$)$_3$](PF$_6$)$_2$** several significant differences can be evidenced: (*i*) a red shift of IL and MLCT bands (λ_{IL} = 266 and 263 nm, and λ_{MLCT} around 454 and 445 nm for **[Ru(phen-NH$_2$)$_3$](PF$_6$)$_2$** and **[Ru(phen)$_3$](PF$_6$)$_2$**, respectively); (*ii*) a decrease of the extinction molar coefficient for IL transitions; (*iii*) an intense and broad band around 365 nm corresponding to a low energy ILCT transition from NH_2 function to the π_{Phen}^* (see Table S3, transitions $S_0 \rightarrow S_n$ with n = 33-36). For complexes with phen-NH_2 ligands, the intensity of this ILCT absorption band is directly proportional to the number of **phen-NH$_2$** ligand (see Figure 6, Table 3, and also Figure S15 and S16 in the ESI).

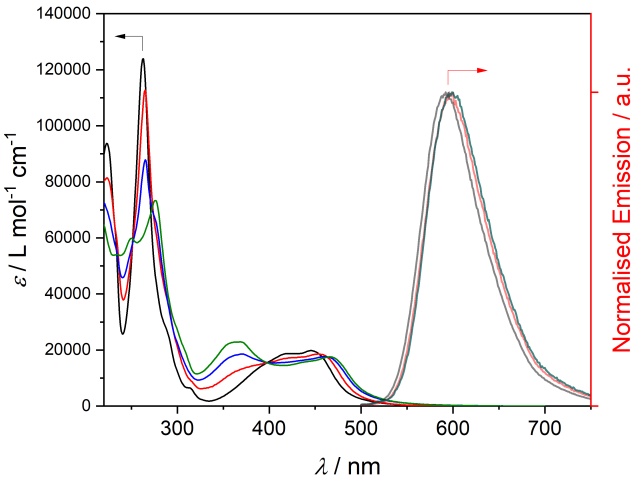

Figure 6. Absorption in molar extinction coefficient and normalised luminescence spectra (λ_{exc} = 450 nm) at room temperature in acetonitrile of **[Ru(phen)$_3$](PF$_6$)$_2$** (black/grey), **[Ru(phen)$_2$(phen-NH$_2$)](PF$_6$)$_2$** (red/light red), **[Ru(phen)(phen-NH$_2$)$_2$](PF$_6$)$_2$** (blue/light blue), and **[Ru(phen-NH$_2$)$_3$](PF$_6$)$_2$** (green/light green).

The presence of one **phen-X** ligand has an important influence on the photophysical properties of the related heteroleptic **[Ru(phen)$_2$(phen-X)](PF$_6$)$_2$** complexes (see Fig. 7). For X being an electro-withdrawing group (cyano and epoxide), a large decrease of the MLCT intensity is observed compared to the reference complex **[Ru(phen)$_3$](PF$_6$)$_2$** without notable change of the absorption wavelength. When X is an electro-releasing group (-NH$_2$), and like for the homoleptic complexes, there is also a decrease in the intensity of this band which is between the ones observed for **[Ru(phen)$_3$](PF$_6$)$_2$** and for the heteroleptic complexes with an electro-withdrawing group. An important ILCT transition is confirmed on the **[Ru(phen)$_2$(phen-NH$_2$)](PF$_6$)$_2$** spectrum (see Figure 6 as well as Figure S16 and Table S2, transition $S_0 \rightarrow S_n$ with n = 24). Such an intense ILCT band involving a X → phen charge flow is not present on the spectra related to the heteroleptic complexes bearing an electro-withdrawing group. For the heteroleptic complexes [Ru(phen)$_2$(phen-X)]$^{2+}$ (X = NH$_2$, CN), MLCT transition of weak intensities are found to contribute to the low-energy part of their visible absorption band (see Table S2, Fig. S16 and Table S4, Fig. S17 for X = NH$_2$ and CN, respectively).

Emission Spectroscopy. In order to characterize the ^{3}MLCT of our complexes, luminescence spectra were measured in acetonitrile and all consisted in a broad band centred around 600 nm (see Figure 5, 6 and 7). The maxima wavelengths (λ_{em}), quantum yield (ϕ) and related excited-state lifetimes (τ) are presented Table 3, and are in good agreement with the emission from the ^{3}MLCT excited-state. The nature of the substituent at the fifth position of the 1,10-phenanthroline has a small impact on the emission spectral range. A red shift is observed for the electron-donating complexes **[Ru(phen)$_2$(phen-NH$_2$)](PF$_6$)$_2$** and **[Ru(phen)(phen-NH$_2$)$_2$](PF$_6$)$_2$** compared to **[Ru(phen)$_3$](PF$_6$)$_2$** (λ_{em} = 595, 599 and 590 nm, respectively).
However, this bathochromic shift is less pronounced than for the complexes with an electro-withdrawing group in acetonitrile (λ_{em} = 625 nm for **[Ru(phen)$_2$(phen-CN)](PF$_6$)$_2$**, for example, see Figure 7).

Table 3. Photophysical properties of the studied Ru(II) complexes in deaerated acetonitrile.

	λ_{abs} / nm (ε /10^4 L mol^{-1} cm^{-1})	λ_{em} /nm	ϕ	τ /ns (χ^2)	k_r / 10^4 s^{-1}	k_{nr} / 10^6 s^{-1}	k_r / k_{nr}	λ_{2PA} max / nm (σ_{2PA} max / GM)
[Ru(phen)$_3$](PF$_6$)$_2$	263 (12.40) 420 (1.87) 445 (1.98)	590	0.04	890 (1.089)	4.5	1.12	0.04	750 (20) 850 (10) 930 (10)
[Ru(phen)$_2$(phen-X)](PF$_6$)$_2$								
X = NH$_2$	266 (11.07) 418 (1.70) 454 (1.86)	595	0.05	850 (1.118)	5.9	1.11	0.05	750 (32)
X = epoxide	265 (8.88) 422 (1.38) 450 (1.50)	610	0.08	850 (1.082)	9.4	1.08	0.08	750 (55)
X = CN	264 (10.70) 422 (1.45) 447 (1.62)	625	0.11	1780 (1.090)	6.2	0.50	0.12	740 (30)
[Ru(phen)(phen-X)$_2$](PF$_6$)$_2$								
X = NH$_2$	265 (7.80) 370 (1.65) 461 (1.57)	599	0.08	1000 (1.133)	8.0	0.92	0.09	750 (35)
[Ru(phen-X)$_3$](PF$_6$)$_2$								
X = NH$_2$	276 (7.33) 365 (2.29) 466 (1.76)	597	0.11	1980 (1.048)	5.5	0.45	0.12	760 (42)
X = CN	265 (11.43) 422 (1.65) 447 (1.85)	603	0.06	1010 (1.074)	5.9	0.93	0.06	760 (53)

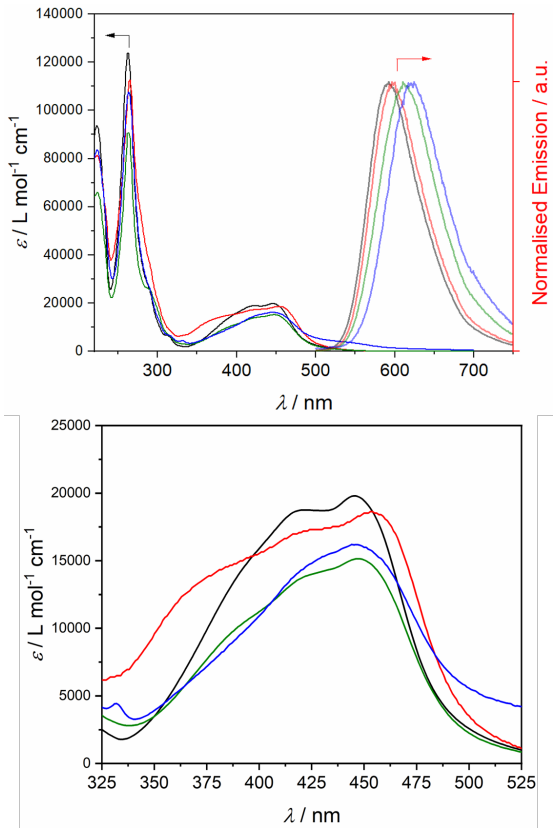

Figure 7. *top*: Absorption and normalised luminescence spectra at room temperature (λ_{exc} = 450 nm) in acetonitrile of **[Ru(phen)$_3$](PF$_6$)$_2$** (black grey) and of heteroleptic complexes **[Ru(phen)$_2$(phen-NH$_2$)](PF$_6$)$_2$** (red/light red), **[Ru(phen)$_2$(phen-epoxide)](PF$_6$)$_2$** (green/light green), **[Ru(phen)$_2$(phen-CN)](PF$_6$)$_2$** (blue/light blue); *bottom*: zoom on the

320-520 spectral range.

From the experimental data (quantum yield ϕ and excited-state lifetime τ), the k_r (radiative decay rate) and k_{nr} (non radiative decay rate) values were obtained. The ϕ and the related (quite similar) k_r/k_{nr} values, increase as the number of π*-acceptor ligand (L) involved in the metal-to-ligand L charge transfer (MLCT) decreases. Concerning complexes involving electro-releasing group (**$[Ru(phen)_{3-n}(phen\text{-}NH_2)_n](PF_6)_2$** as example in this study), quantum yield ϕ is determined as 0.04, 0.05, 0.08 and 0.11 for n=0, 1, 2 and 3, respectively. This can be quite perfectly correlated with the related decreasing of the non radiative processes (k_{nr} = 1.12, 1.11, 0.92 and 0.45 10^6 s^{-1} for n=0, 1, 2 and 3, respectively). The reverse situation is observed with strong electro-withdrawing substituents and ϕ = 0.11 and 0.06 for n=1 and 3, respectively. The emission properties based on these MLCT type excited-state are improved as they are close to a mono-directional transfer, reducing the possibilities of non radiative relaxation. These results are also in good agreement with reported literature claiming that drastic differences in emission properties are due to the localization (and ligand(s) involved) of the lowest ^{3}MLCT.[42]

The dependence of the Stokes shifts $\Delta\nu_{ST}$ (defined as the loss of energy between absorption and emission of light) with the solvent orientation polarizability Δ_f (defined according to the static dielectric constant ε and refractive index n of the solvent, see equation 1) was studied using the Lippert-Mataga plot[43]. This correlation (Eq. 3) is the most widely used equation to describe the effects of the physical properties of the solvent on the emission spectra of luminophores.

$$\Delta\nu_{ST} = \Delta\nu_{ST}^0 + \left[\frac{2}{(4\pi\varepsilon_0)(hca^3)}\right](\mu_e-\mu_g)^2\Delta f(\varepsilon,n) \quad (3)$$

with $$\Delta f(\varepsilon,n) = \frac{\varepsilon-1}{2\varepsilon+1} - \frac{n^2-1}{2n^2+1}$$

a is the value of the Onsager cavity radius in which the fluorophore resides, h is the Planck's constant, c the celerity of the light, ε_0 is the vacuum permittivity and μ_e and μ_g are the excited-state and ground-state dipole moments, respectively. As illustrated in Figure 8 and Figure S18 for the example of $[Ru(phen)_{3-n}(phen\text{-}NH_2)_n](PF_6)_2$ family, a small dependence of the maximum emission wavelengths with the solvent polarity was evidenced and nearly no difference was observed in the UV-visible absorption spectra. This observation would suggest that the fluorescence properties are due to the radiative relaxation of an excited-state with a small increase of the dipole moment compared to the ground state.

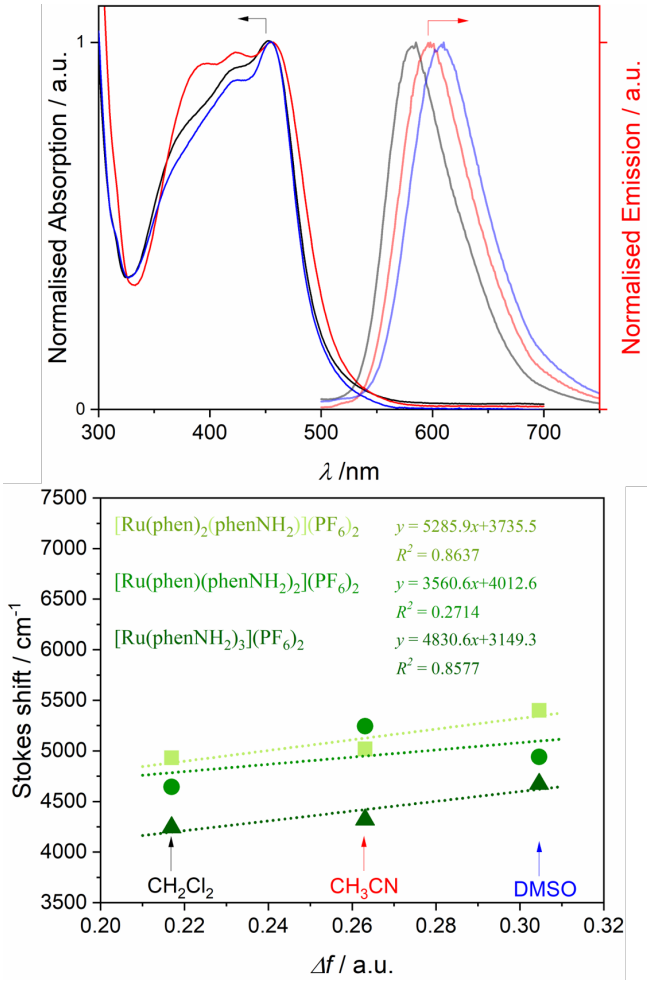

Figure 8. Absorbance and emission spectra in CH_2Cl_2 (black/grey), CH_3CN (red/light red) and DMSO (blue/light blue) (λ_{exc} = 450 nm) of **[Ru(phen)$_2$(phen-NH$_2$)](PF$_6$)$_2$**, plotted here as an example representative of the series.; *bottom*, Plot of the Stokes Shift ($\Delta\nu_{ST}$) against the solvent orientation polarizability Δf parameter of the same solvents for **[Ru(phen)$_2$(phen-NH$_2$)](PF$_6$)$_2$** (light green), **[Ru(phen)(phenNH$_2$)$_2$](PF$_6$)$_2$** (green) and **[Ru(phenNH$_2$)$_3$](PF$_6$)$_2$** (dark green).

For the same family of complexes, Figure 9, reporting the bathochromic shift (in cm^{-1}) of the emission in dichloromethane to DMSO according to the number of phen-NH_2 ligands, is in good agreement with a decrease of the dipolar moment of the excited-state going from **[Ru(Phen)$_2$(Phen-NH$_2$)]$^{2+}$** to the more symmetric one **[Ru(Phen-NH$_2$)$_3$]$^{2+}$**.

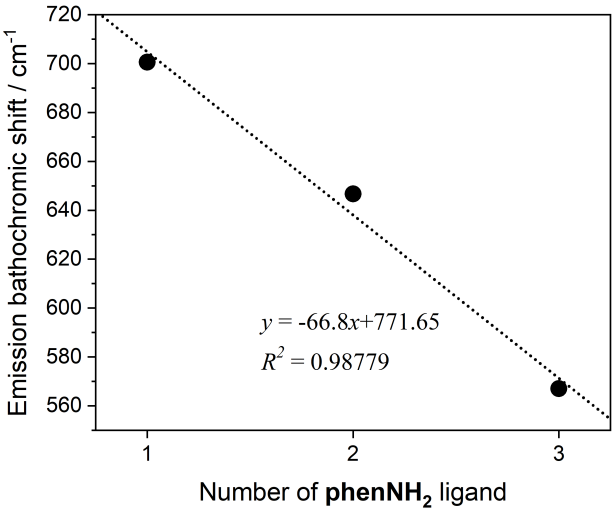

Figure 9. Bathochromic shift observed for the emission of $[Ru(Phen)_{3-n}(Phen\text{-}NH_2)_n](PF_6)_2$ (in cm^{-1}) from dichloromethane to DMSO, according to the number *n* of phen-NH_2 ligand(s).

Nonlinear optical properties. Two-photon absorption (2PA) properties in the MLCT spectral range are of interest for potential applications in optical power limiting in the near infrared, biological imaging, and photodynamic therapy for example.[44] Several studies were already carried out on MLCT transitions by 2PA at a single wavelength (750, 800 and 880 nm) for ruthenium(II)[45,22] and rhenium(I)[46] complexes or Z-scan experiments giving rise to two-photon transitions spectra.[47] Two photons absorption efficiencies of the family of complexes involving the ligand phen-NH_2 (from 0 to 3 ligands) were measured between 700 and 1000 nm and compared to the linear spectra (Figure 10). A maximum is observed around 750-760 nm which corresponds mainly to the ILCT transition of the different complexes studied whereas the lowest energy MLCT transition is almost forbidden in two-photon absorption with a two photon absorption cross-section σ_{2PA} between 7 and 10 GM at 900 nm (1 GM = 10^{-50} cm^4.s.photons^{-1}). It has to be pointed out that it is even relatively less allowed for the compounds exhibiting the highest symmetry (see Figure 10 *top*, and spectra around 900 nm for **$[Ru(phen)_3](PF_6)_2$** and **$[Ru(phen\text{-}NH_2)_3](PF_6)_2$**). It is also important to notice that the other MLCT broad band (around 410 nm for the linear absorption) is more allowed in its two-photon transition with a shoulder recorded at around 820 nm and 2PA absorption efficiency (from around 10 to 30 GM) directly related to the increasing number of electro-donating NH_2 group. The most efficient complex in 2PA is found to be the **$[Ru(phen\text{-}NH_2)_3](PF_6)_2$** with a σ_{2PA} of 42 GM (at 760 nm), highlighting the importance of rationalising the design of the ligand to increase the lower cross-section observed for the parent **$[Ru(phen)_3](PF_6)_2$** (25 GM at 760 nm). Moreover, the σ_{2PA} increased in a linear fashion with the **phen-NH_2** ligand content of the complexes as observed in the **$[Ru(phen)_{3-n}(phen\text{-}NH_2)_n](PF_6)_2$** series (n = 0 -3, Figure 10, *bottom*). These results are in good agreement with the similar evolution of the intensity of the ILCT transition in the linear absorption spectra also plotted in Figure 10 (*bottom*). As for the one-dimensional analogues, the amount of charge transferred from the ground state to the excited state (and the related difference in state dipole moment) is the most relevant parameters to achieve high σ_{2PA} values.[16c]

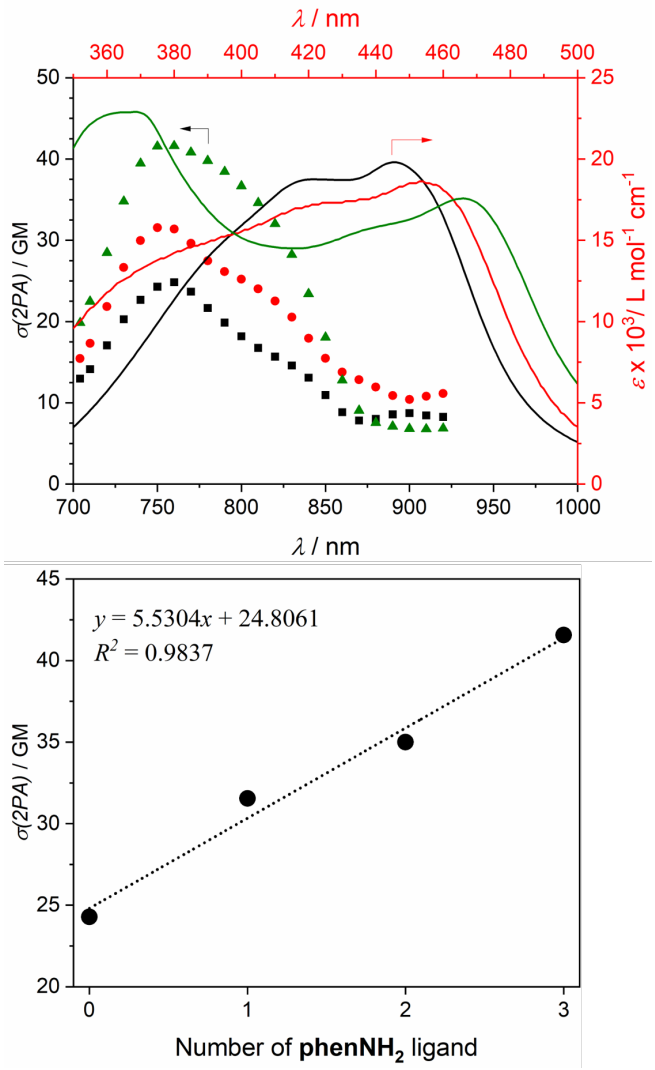

Figure 10. *top*, Two-photon absorption cross-section (σ_{2PA}, dots, in G.M. units = 10^{-50} $cm^4.s.photon^{-1}$) and linear absorption (plain lines) at room temperature in acetonitrile for **[Ru(phen)$_3$](PF$_6$)$_2$** (black), **[Ru(phen)$_2$(phen-NH$_2$)](PF$_6$)$_2$** (red) and **Ru(phen-NH$_2$)$_3$](PF$_6$)$_2$** (green); *bottom*, linear correlation between the number of **phen-NH$_2$** ligand(s) in the complex and the two-photon absorption cross-sections measured at 750 nm.

Conclusion

A series of substituted 1,10-phenanthroline-based Ru(II) complexes have been synthetized and characterized. 1,10-phenanthroline ligands were substituted in the fifth position by either electro-donating (X = NH_2) or withdrawing groups (X = epoxy, CN). Although the synthesis of the homoleptic and $[Ru(phen)_2(phen\text{-}X)]^{2+}$ heteroletptic complexes followed usual procedures, we propose here a quite easy way to access the other heteroleptic $[Ru(phen)_2(phen\text{-}X)]^{2+}$ complex in a one-pot reaction. The joint electrochemical and DFT theoretical investigation highlighted the possibility to predict redox potentials of 5-substituted-1,10-phenanthroline-based Ru(II) complexes as functions of their calculated HOMO and LUMO energies. Such model can be used to predict the electronic properties (redox potentials, photo-physical characteristics) depending either on the nature of the substitution of the ligand or the symmetry of the related homo- or heteroleptic complexes (most probably analysed for this study as a mixture of diastereoisomers). The nature of the transitions in linear absorption

spectroscopy were determined by the mean of TD-DFT analysis, allowing the identification of the ILCT bands to be the best qualitative indicator of the two-photon absorption properties in a series of **$[Ru(phen)_{3-n}(phen\text{-}NH_2)_n](PF_6)_2$** coordination complexes (n = 0-3). Following the trend in their respective ILCT band intensities, the homoleptic complex **$[Ru(phen\text{-}NH_2)_3](PF_6)_2$** showed the best 2PA properties among the series, with a σ_{2PA} of 42 GM (at 760 nm). Such prediction and control over the fine-tuning of optical properties in ruthenium complexes is of interest for potential applications in photovoltaic devices, as photosensitizers in photoredox catalysis or photodynamic therapy (PDT), where Ru(II) remains one of the most highly studied and efficient metal ion.

Experimental Section

General: Reactions were performed under an argon inert atmosphere using standard Schlenk-line techniques unless otherwise stated. All reagents were purchased from commercial sources and used without further purification.

Instrumentation: ^{1}H and ^{13}C NMR spectra were recorded with a Bruker AC FT NMR spectrometer (at 250.1 MHz for ^{1}H and 62.9 MHz for ^{13}C). Elemental analyses were carried out on a Perkin-Elmer 2400. Samples were also analysed by ESI/Q-ToF HRMS method, performed on a Waters SYNAPT G2-Si High Resolution Mass Spectrometry equipped with electrospray ionization (ESI) source. UV/Vis and emission spectra were recorded respectively on a Cary 5000 UV-2401PC spectrophotometer and a Varian Cary Eclipse spectrofluorometer. Infrared spectra were recorded on a Nicolet IS5 spectrometer equipped with an ATR ID5 module. Cyclic voltammetry was performed on a Radiometer PST006 potentiostat using a conventional three-electrodes cell in acetonitrile containing 0.1 M Bu_4NPF_6 as supporting electrolyte. The saturated calomel electrode (SCE) was separated from the test compartment using a bridge tube. The solutions of studied complexes (0.5 mM) were purged with argon before each measurement. The working electrode was a 1 cm^2 glassy carbon disc, the counter-electrode a Pt wire and the reference electrode. After the measurement, ferrocene was added as an internal reference for calibration. In these conditions the redox potential of the couple Fc^+/Fc was found equal to 0.39 V. All potentials are quoted *versus* SCE. In all the experiments the scan rate was 100 mV/s.

Time-resolved luminescence measurements were performed on deoxygenated dilute solutions of acetonitrile (*ca.* 10^{-6} M, optical density < 0.1) contained in 1 cm airtight quartz cuvettes using an Edinburgh Instruments (FLS920) spectrometer in photon-counting mode. Fully corrected emission spectra were obtained, for each compound, at $\lambda_{ex} = \lambda_{max}^{abs}$ with an optical density at $\lambda_{ex} \leq 0.1$ to minimize internal absorption. Luminescence lifetimes were measured by time correlated single-photon counting (TCSPC) by using the same FLS 920 fluorimeter. Excitation was achieved by a hydrogen-filled nanosecond flashlamp (repetition rate 40 kHz). The instrument response (FWHM ca. 1 ns) was determined by measuring the light scattered by a Ludox suspension. The TCSPC traces were analyzed by standard iterative reconvolution methods implemented in the software of the fluorimeter. All compounds displayed monoexponential decays (χ^2<1.15).

The two-photon absorption spectra of the complexes and the ligands were determined in the 700–930 nm range by investigating their two-photon excited luminescence (2PEL) in deoxygenated 10^{-4} M acetonitrile

solutions. The measurements were performed using a Nd:YLF-pumped Ti:sapphire oscillator generating 150 fs pulses at a 76 MHz rate. The excitation was focused into the cuvette through a microscope objective (10x, NA 0.25). The luminescence was detected in epifluorescence mode via a dichroic mirror (Chroma 675dcxru) and a barrier filter (Chroma e650sp-2p) by a compact CCD spectrometer module BWTek BTC112E. Total luminescence intensities were obtained by integrating the corrected emission spectra measured by this spectrometer. 2PA cross-sections (σ_{2PA}) were determined from the two-photon excited luminescence cross-sections ($\sigma_{2PA}\Phi$) and the luminescence emission quantum yield (Φ). 2PEL cross-sections of 10^{-4} M solutions were measured relative to a 10^{-4} M solution of fluorescein in 0.01 M aqueous NaOH. The quadratic dependence of the luminescence intensity on the excitation power was checked for each sample and all wavelengths.

Computational details. Density functional theory (DFT)[38b] has been applied to the optimization of the geometries of the homoleptic $[Ru(L)_3]^{2+}$ (L = phen, phen-NH_2, phen-CN) and heteroleptic $[Ru(phen)_2(L)]^{2+}$ (L = Phen-NH_2, Phen-CN) complexes. The optimizations have been performed with the ADF program package[50], using the PBE exchange-correlation energy functional[51] combined with the TZ2P Slater-type (STO) basis set of triple-ζ doubly polarized quality from the ADF basis set database[40]. The atomic core levels were kept frozen up to the 3d level for the Ru atom, and up to the 1s level for the N and C atoms. The absorption spectra of the complexes in acetonitrile have been characterized by computing potential the energies and oscillator strengths of their 100 lowest-lying electronic excitations within linear response theory in time-dependent DFT (TDDFT) as implemented in ADF[39]. The statistical average of orbital potentials (SAOP)[52] exchange-correlation potential and the all-electron TZ2P basis set were employed for the electronic excitation calculations. All calculations were run spin-restricted and scalar relativistic (SR) effects were included within the zero order regular approximation (ZORA).[53]

Ligand synthesis. All the ligands involved in the complex synthesis were obtained according to procedures described in the literature.[25,26]

Complex synthesis:

$[Ru(phen)_2(phen\text{-}NH_2)](PF_6)_2$: In a 50 mL three-necked flask under argon, 94 mg of 5-amino-1,10-phenanthroline (0.48 mmol, 1.1 eq.) were added tot 230 mg of **$[Ruphen_2Cl_2]$** (0.43 mmol) dissolved in 18 mL of DMF. The mixture was heated at reflux overnight. Saturated aqueous solution of NH_4PF_6 was added to the solution at room temperature. The resulting precipitate was collected by filtration, washed three times by water, and three times by diethyl ether. 366 mg of a dark red powder was obtained (yield = 90%). ^{1}H NMR (250 MHz, $(CD_3)_2CO$): δ (ppm): 8.93 (d, 1H, ^3J = 8.5 Hz); 8.83-8.77 (m, 4H); 8.44-8.32 (m, 10H); 7.97-7.74 (m, 6H) ; 7.54-7.50 (m, 1H) ; 7.31 (s, 1H); 6.43-6.41 (m, 2H, N*H*$_2$). IR (ATR) σ (cm^{-1}): 3390, 1636, 1594, 1426, 834, 724, 556. Anal. calcd for $RuC_{36}H_{25}N_7P_2F_{12}$, 2 H_2O (%): C, 44.0; H, 2.9; N, 10.0. Found (%): C, 43.6; H, 2.5; N, 10.2. HRMS: calcd for $RuC_{36}H_{25}N_7PF_6$: 802.0857 [M^+]; found: 802.0581.

$[Ru(phen)_2(phen\text{-}epoxide)](PF_6)_2$: 1,10-phenanthroline, monohydrate (194 mg, 0.98 mmol, 2 eq.) dissolved in 50 mL of ethanol was degassed with $Ar_{(g)}$ for 20 min followed by the addition of 250 mg of **$[Ru(dmso)_4Cl_2]$** (0.516 mmol, 1 eq.). The mixture was heated at reflux under argon and in the dark overnight. After cooling down the reaction mixture to room temperature, 100 mg of 5,6-epoxide-1,10-phenanthroline (0.52 mmol, 1 eq.) were

added. The mixture was heated again at reflux under an argon atmosphere, and in the dark overnight. A saturated aqueous solution of NH_4PF_6 was added at room temperature to precipitate the desired product. The brown precipitate was collected by filtration, washed three times with water, two times with diethyl ether and dried under vacuum. The product obtained was solubilized in a minimum amount of acetone and was precipitated in ethanol to give 300 mg of brown powder (yield = 30%). ^{1}H NMR (250 MHz, $(CD_3)_2CO$): δ (ppm): 8.92-8.67 (m, 6H), 8.52-8.32 (m, 11H), 7.88-7.68 (m, 5H), 5.11 (s, 1H). ^{13}C NMR (62.9 MHz, $(CD_3)_2CO$): δ (ppm): 154.02, 153.85, 153.20, 148.93, 139.87, 139.72, 137.83, 131.97, 129.08, 128.55, 128.34, 127.36, 127.08, 55.86, 55.74. IR (KBr pellets) σ (cm^{-1}): 3423, 3086, 1625, 1427, 841, 722, 557. Anal. calcd for $RuC_{36}H_{24}N_6OP_2F_{12}$, 1 H_2O (%): C, 44.8; H, 2.7; N, 8.7. Found (%): C, 44.8; H, 2.7; N, 8.7. HRMS: calcd for $RuC_{36}H_{24}N_6O$: 658.1112 [M^+]; found: 658.1060.

[Ru(phen)$_2$(phen-CN)](PF$_6$)$_2$: **[Ru(phen)$_2$Cl$_2$]** (390 mg, 0.73 mmol) dissolved in 28 mL of DMF was mixed with 5-cyano-1,10-phenanthroline (150 mg, 0.74 mmol) under argon. The mixture was vigorously stirred at reflux overnight. A saturated aqueous solution of NH_4PF_6 was added at room temperature to precipitate the desired product after stirring for 2h. The dark orange precipitate was collected by filtration, washed three times with water (10 mL) and twice with diethyl ether (10 mL). The crude product was recrystallized in a mixture of acetone/ethanol and dried under vacuum. (591 mg, yield = 85 %). ^{1}H NMR (250 MHz, $(CD_3)_2CO$): δ (ppm): 9.13 (s, 1H), 8.93-8.78 (m, 6H), 8.62-8.58 (m, 2H), 8.46-8.38 (m, 7H), 8.01-7.89 (m, 3H), 7.83-7.77 (m, 4H). IR (KBr pellets) σ (cm^{-1}): 3410, 3065, 2231, 1977, 1629, 1427, 854, 721, 557. Anal. calcd for $RuC_{37}H_{23}N_7P_2F_{12}$, 1.5 H_2O (%): C, 45.2; H, 2.7; N, 10.0. Found (%): C, 45.6; H, 2.3; N, 9.7. HRMS: calcd for $RuC_{37}H_{23}N_7PF_6$: 812.0710 [M^+]; found: 812.0700.

[Ru(phen)(phen-NH$_2$)$_2$](PF$_6$)$_2$: 5-amino-1,10-phenanthroline (32.5 mg, 0.166 mmol) dissolved in 5 mL of ethanol was degassed with $Ar_{(g)}$ for 20 min. followed by the addition of 40.4 mg of **[Ru(dmso)$_4$Cl$_2$]** (0.083 mmol, 0.5 eq.). The mixture was heated at reflux under argon and in the dark overnight. After cooling down the reaction mixture to room temperature, 16 mg of 1,10-phenanthroline (0.088 mmol, 0.5 eq.) were added. The mixture was heated again at reflux under inert atmosphere and in the dark overnight. A saturated aqueous solution of NH_4PF_6 was added at room temperature to precipitate the desired product after stirring for 2h. The orange precipitate was collected by centrifugation, washed three times with water and twice with diethyl ether. The product obtained was solubilized in a minimum amount of acetone, precipitated in ethanol and dried on vacuum yielding 27.5 mg of brown powder (yield = 30%). ^{1}H NMR (250 MHz, $(CD_3)_2CO$): δ (ppm): 8.94-8.80 (m, 4H), 8.40-8.35 (m, 8H), 7.93-7.77 (m, 6H), 7.55 (br, 2H), 7.30 (s, 2H), 6.39 (s, 2H). ^{13}C NMR (62.9 MHz, $(CD_3)_2CO$): δ (ppm): 153.92, 153.53, 149.63, 148.90, 148.57, 145.79, 143.03, 137.66, 137.53, 134.38, 134.24, 133.80, 132.29, 132.16, 131.89, 129.02, 127.02, 126.68, 125.61, 124.74, 103.79. IR (ATR) σ (cm^{-1}): 3393, 1637, 1512, 1425, 836, 722, 557. Anal. calcd for $RuC_{38}H_{30}N_8P_2F_{12}O_{4.25}S_{0.25}$ 4 H_2O, 0.25 DMSO (%): C, 42.7; H, 3.7; N, 10.4; S, 0.7. Found (%): C, 42.6; H, 3.3; N, 9.9: S, 0.6. HRMS: calcd for $RuC_{36}H_{26}N_8$: 672.1300 [M^+]; found: 672.1326

[Ru(phen-NH$_2$)$_3$](PF$_6$)$_2$: 5-amino-1,10-phenanthroline (257 mg, 1.32 mmol) dissolved in 46 mL of ethanol was degassed with argon for 20 min. followed by the addition of 213 mg of **[Ru(dmso)$_4$Cl$_2$]** (0.44 mmol, 0.33 eq.). The mixture was heated at reflux under an argon inert atmosphere and in the dark overnight. A saturated aqueous solution of NH_4PF_6 was added at room temperature to precipitate the desired product after stirring for 2h. The

orange precipitate was collected by filtration, washed three times with water, twice with diethyl ether and dried under vacuum. The crude material was purified on a silica column (eluent CH_3CN/H_2O 90:10:$\varepsilon NaNO_3$), recrystallized in a acetone/pentane mixture and then washed with CH_2Cl_2, yielding 168 mg of powder (yield = 34%). ^{1}H NMR (250 MHz, $(CD_3)_2CO$): δ (ppm): 8.87 (d, 3H, J = 9 Hz), 8.27 (d, 6H, J = 8 Hz), 7.94-7.78 (m, 3H), 7.78-7.66 (m, 3H), 7.57-7.44 (m, 3H), 7.26 (s, 3H), 6.39 (s, 1H). IR (ATR) σ (cm^{-1}): 3364, 3397, 3228, 1640, 1512, 1430, 1089, 842, 723, 558. Anal. calcd for $RuC_{36}H_{27}N_9P_2F_{12}$, 4 H_2O, 0.5 NH_4PF_6 (%): C, 37.9; H, 3.2; N, 11.6. Found (%): C, 38.2; H, 2.6; N, 11.3. HRMS: calcd for $RuC_{36}H_{27}N_9$: 687.1400 [M^+]; found: 687.1442

[Ru(phen-CN)$_3$](PF$_6$)$_2$: 5-cyano-1,10-phenanthroline (97 mg, 0.48 mmol) dissolved in 17 mL of ethanol was degassed with $Ar_{(g)}$ for 20 min. followed by the addition of 77 mg of **[Ru(dmso)$_4$Cl$_2$]** (0.16 mmol, 0.33 eq.). The mixture was heated at reflux under an $Ar_{(g)}$ inert atmosphere and in the dark overnight. A saturated aqueous solution of NH_4PF_6 was added at room temperature to precipitate the desired product after stirring for 2h. The orange precipitate was collected by filtration, washed three times with water, three times with diethyl ether and once with hexane, yielding 123 mg of a brownish powder (yield = 70%). ^{1}H NMR (250 MHz, $(CD_3)_2CO$): δ (ppm): 9.16 (s, 3H), 8.90 (dd, 6H, J = 16.50, 8.00 Hz), 8.61 (d, 6H, J = 5 Hz), 8.04-7.08 (m, 6H). IR (ATR) σ (cm^{-1}): 3646, 3086, 2230, 1427, 841, 726, 557. Anal. calcd for $RuC_{39}H_{21}N_9P_2F_{12}$, 1.75 H_2O, 0.25 NH_4PF_6, 0.1 DMSO (%): C, 43.3; H, 2.4; N, 11.9; S, 0.3. % Found (%): C, 43.8; H, 2.1; N, 11.4: S, 0.4. HRMS: calcd for $RuC_{39}H_{21}N_9$: 717.1000 [M^+]; found: 717.0966

ACKNOWLEDGEMENTS

Part of this work was supported by ANR funding (PRC-CE07-033 *IsoGate* Grant).

REFERENCE

1 A. Juris, V. Balzani, F. Barigelletti, S. Campagna, P. Belser and A. Von Zelewsky, *Coord. Chem. Rev*. 1988, **84**, 85.

2 J. V. Caspar and T.J. Meyer, *J. Am. Chem. Soc*., 1983, **105**, 5583.

3 (a) M. G. Humphrey, B. Lockhart-Gillet, M. Samoc, B. W. Skelton, V.-A. Tolhurst, A. H. White, A. J. Wilson and B. F. Yates, *J. Organomet. Chem.* 2005, **690**, 1487; (b) C. E. Powell, M. P. Cifuentes, M. G. Humphrey, A.C. Willis, J. P. Morrall and M. Samoc, *Polyhedron* **2007**, *26*, 284; (c) T. V. Duncan, P. R. Frail, I. R. Miloradovic and M. J. Therien, *J. Phys. Chem. B,* 2010, **114**, 14696; (d) M. Four, D. Riehl, O. Mongin, M. Blanchard-Desce, L. M. Lawson-Daku, J. Moreau, J. Chauvin, J. A. Delaire and G. Lemercier, *PhysChemChemPhys.* 2011, **13**, 17304; (e) C. Girardot, B. Cao, J.-C. Mulatier, P. L. Baldeck, J. Chauvin, D. Riehl, J. A. Delaire, C. Andraud and G. Lemercier, *ChemPhysChem.,* 2008, **9**, 1531.

4 (a) P. Hartmann, W. Ziegler, *Anal. Chem*. 1996, **68**, 4512; (b) B. Elias and A. Kirsch-De Mesmaeker, *Coord. Chem. Rev*. 2006, **250***,* 1627.

5 (a) L. Tan-Sien-Hee, L. Jacquet and A. Kirsch-De Mesmaeker, *J. Photochem. Photobiol. A : Chem*. 1994, **81**, 169; (b) A. A. Abdel-Shafi, P. D. Beer, R. J. Mortimer and F. Wilkinson, *PhysChemChemPhys* 2000, **2**, 3137; (c) A. A. Abdel-Shafi, P. D. Beer, R. J. Mortimer and F. Wilkinson, *J. Phys. Chem. A*. 2000, **104**, 192; (d) F. Schmitt, P. Govndaswamy, G.Süss-Fink, W. H.; Ang, P. J. Dyson, L. Juillerat-Jeanneret and B. Therrien, *J. Med. Chem*. 2008, **51**, 1811; (e) Y. Liu,; R. Hammitt, D. A. Lutterman, L. E. Joyce, R. P. Thummel and C. Turro, *Inorg. Chem*. 2009, **48,** 375; (f) C. Boca, M. Four, A. Bonne, B. van Der Sanden, S. Astilean P. L. Baldeck and G. Lemercier, *Chem. Commun.* 2009, 4590.

6 (a) K. Sénéchal, O. Maury, H. Le Bozec, I. Ledoux and J. Zyss, *J. Am. Chem. Soc.*, 2002, **124**, 4560; (b) B. J. Coe, *Acc. Chem. Res.,* 2006, **39**, 383; O. Maury and H. Le Bozec, *Acc. Chem. Res*., 2005, **38**, 691.

7 T. G. Goodson, III, *Acc. Chem. Res*. 2005, **38**, 99; Y. Wang, G. S. He, P. N. Prasad and T. Goodson, III, *J. Am. Chem. Soc*. 2005, **127**, 10128.

8 C. Katan, F. Terenziani, O. Mongin, M. H. V. Werts, L. Porrès, T. Pons, J. Mertz, S. Tretiak and M. Blanchard-Desce, *J. Phys. Chem. A*, 2005, **109**, 3024.

9 O. Maury, L. Viau, K. Sénéchal, B. Corre, J.-P. Guégan, T. Renouard, I. Ledoux, J. Zyss and H. Le Bozec, *Chem. Eur. J.*, 2004, **10**, 4454.

10 M. Samoc, N. Gauthier, M. P. Cifuentes, F. Paul, C. Lapinte and M. G. Humphrey, *Angew. Chem. Int. Ed*. 2006, **45**, 7376.

11 (a) B. A. Reindhardt, *Photonics Science News* 1999, 21; (b) Marder S. R. *Chem. Comm*. 2006, 131.

12 H. J. D. Bhawalkar, N. D. Kumar, C. F. Zhao and P. N. Prasad, *J. Clin. Med. Surg*., 1997, **15**, 201; J. Liu, Y. W. Zhao, J. Q. Zhao, A. D. Xia, L. J. Jiang, S. Wu, L. Ma, Y. Q. Dong and Y. H. Gu, *J. Photochem. Photobiol. B*, 2002, **68**, 156; K. Ogawa, H. Hasegawa, Y. Inaba, Y. Kobuke, H. Inouye, Y. Kanemitsu, E. Kohno, T. Hirano, S. I. Ogura and I. Okura, *J. Med. Chem*., 2006, **49**, 2276.

13 (a) W. Denk, J.H. Strickler and W.W. Webb, *Science*, 1990, **248**, 73; (b) Y. Shen, D. Jakubczyk, F. Xu, J. Swiatkiewicz, P. N. Prasad and B. A. Reinhardt, *Appl. Phys. Lett*., 2000, **76**, 1.

14 (a) B. H. Cumpston, S. P. Ananthavel, S. Barlow, D.-L. Dyer, J. E Ehrlich, L.L. Erskine, A. A. Heikal, S. M. Kuebler, I.-Y.S. Lee, D. McCord-Maughon, J. Qin, H. Röckel, M. Rumi, X.-L. Wu, S. R. Marder and J. W. Perry, *Nature*, 1999, **398**, 51; (b) S. Kawata, H.-B. Sun, T. Tanaka and K. Takada, *Nature*, 2001, **412**, 697; (c) W. Zhou, S. M. Kuebler, K. L. Braun, T. Yu, J. K. Cammack, C. K. Ober, J. W. Perry and S. R. Marder, *Science*, 2002, **296**, 1106.

15 J. E. Ehrlich, X.-L. Wu, I.-Y. S. Lee, Z.-Y. Hu, H. Röckel, S. R. Marder and J.W. Perry, *Opt. Lett.*, 1997, **22**, 1843.

16 (a) M. Albota, D. Beljonne, J.-L. Brédas, J. E. Ehrlich, J.-Y. Fu, A. A. Heikal, S. E. Hess, T. Kogej, M. D. Levin, S. R. Marder, D. McCord-Maughon, J. W. Perry, H. Röckel, M. Rumi, G. Subramaniam, W. W. Webb, X.-L. Wu and C. Xu, Science 1998, **281**, 1653; (b) M. Rumi, J. E. Ehrlich, A. A. Heikal, J. W. Perry, S. Barlow, Z.-Y. Hu, D. McCord-Maughon, T. C. Parker, H. Rçckel, S. Thayumanavan, S. R. Marder, D. Beljonne and J.-L. Brédas, *J. Am. Chem. Soc*. 2000, **122**, 9500; (c) D. Beljonne, W. Wenseleers, E. Zojer, Z. Shuai, H. Vogel, S. J. K. Pond, J. W. Perry, S. R. Marder and J.-L. Brédas, *Adv. Funct. Mater*. 2002, **12**, 631.

17 (a) A. M. McDonagh, M. G. Humphrey, M. Samoc, B. Luther-Davies, *Organometallics,* 1999*,* **18***, 25,* 5195-5197; (b) M. Samoc, J. P. Morrall, G. T. Dalton, M. P. Cifuentes and M. G. Humphrey, *Angew. Chem. Int. Ed.* 2007, **46**, 731-733; (c) G. Lemercier, A. Bonne, M. Four, L. M. Lawson-Daku, *C. R. Chimie* 2008, **11**, 709.

18 M. P. Cifuentes, C. E. Powell, J. P. Morrall, A. M. McDonagh, N. T. Lucas, M. G. Humphrey, M. Samoc, S. Houbrechts, I. Asselberghs, K. Clays, A. Persoons and T. Isoshima, *J. Am. Chem. Soc*. 2006, **128**, 10819.

19 S. K. Hurst, M. G. Humphrey, T. Isoshima, K. Wostyn, I. Asselberghs, K. Clays, A. Persoons, M. Samoc, B. Luther-Davies, *Organometallics* 2002**, 21***,* 2024-2026; S.K. Hurst, M. G. Humphrey, J. P. Morrall, M. P. Cifuentes, M. Samoc, B. Luther-Davis, G.A. Heath, A. C. Willis, *J. Organomet. Chem.* 2003, **670**, 56.

20 S. K. Hurst, N.T. Lucas, M. G. Humphrey, T. Isoshima, K. Wostyn, I. Asselberghs, K. Clays, A. Persoons, M. Samoc, B. Luther-Davis, *Inorg. Chim. Acta* 2003, **350**, 62.

21 σ_{2PA} in GM for Göppert-Mayer with 1 G.M. equal 10^{-50} cm^4 s $molecule^{-1}$ $photon^{-1}$.

22 B. J. Coe, M. Samoc, A. Samoc, L. Zhu, Y. Yi, Z. Shuai, *J. Phys. Chem. A* 2007, **111**, 472.

23 C. Feuvrie, O. Maury, H. Le Bozec, I. Ledoux, J. P. Morrall, G. T. Dalton, M. Samoc and M. G. Humphrey, *J. Phys. Chem. A* 2007, **111**, 8980.

24 A. M. McDonagh, M. G. Humphrey, M. Samoc, B. Luther-Davies, S. Houbrechts, T. Wada, H. Sasabe and A. Persoons, *J. Am. Chem. Soc.* 1999**, 121***,* 1405.

25 S. Ji, H. Guo, X. Yuan, X. Li, H. Ding, P. Gai, W. Wu, W. Wu, J. Zhao, *Org. Lett*., 2010, **12**, 2876.

26 (a) B. Higgins and B. A. DeGraff, *Inorg. Chem*., 2005, **44**, 6662; (b) Y. Shen and B. P. Sullivan, *Inorg. Chem*., 1995, **34**, 6235; (c) C. Truillet, F. Lux, J. Moreau, M. Four, L. Sancey, S. Chevreux, G. Boeuf, P. Perriat, C. Frochot, R. Antoine, P. Dugourd, C. Portefaix, C. Hoeffel, M. Barberi-Heyob, C. Terryn, L. Van Gulick, G. Lemercier and O. Tillement, *Dalton Trans*., 2013, **42**, 12410.

27 P. J. Giordano, C.R. Bock, M. S. Wrighton, *J. Am. Chem. Soc.*, 1978, **100**, 6960; J. W. Hackett, C. Turro, *Inorg. Chem*., **1998**; 37, 2039.

28 E. Rousset, I. Ciofini, V. Marvaud, G. S. Hanan, *Inorg. Chem*. 2017, **56**, *16*, 9515.

29 Y. Su, M. L. Machala and F. N. Castellano, *Inorg. Chim. Acta*, 2010, **363**, 283.

30 R. A. Krause, *Inorg. Chim. Acta*, 1977, **22**, 209.

31 B. A. Moyer, T. J. Meyer, *Inorg. Chem*., 1981, **20**, 436.

32 R. A. Binstead, T. J. Meyer , *J. Am. Chem. Soc.*, 1987, **109**, 3287; F. Barigelletti, A. Juris, V. Balzani, P. Belser, A.Von Zelewsky, *Inorg. Chem*. 1987, **26**, 4115.

33 $E_{1/2}$(Ru(III)/Ru(II)) for **[Ru(phen)$_3$]$^{2+}$** = 1.21 V *vs.* Ag/AgCl reported in S. Bernhard, J. A. Barron, P. L. Houston, H. D. Abruna, J. L. Ruglovksy, X. Gao and G. G. Malliaras, *J. Am. Chem. Soc.* 2002, **124**, 13624.

34 C. Hansch, A. Leo and R. W. Taft, *Chem. Rev.*, 1991, **91**, 165.

35 L. Troian-Gautier and C. Moucheron, *Molecules* 2014, **19**, 5028.

36 C. D. Ellis, L. D. Margerum, R. W. Royce, W. Murray and T. J. Meyer, *Inorg.Chem.* 1983*,* **22***,* 1283.

37 K. L. Brown, X. Hou, O. Banks, K. A. Krueger, J. Hinson, G. F. Peaslee and P. A. DeYoung, *Int. J. Chem*. 2011, **3**, 12.

38 (a) P. Hohenberg and W. Kohn. W. *Phys. Rev*., 1964, **136**, B864. (b) W. Kohn and L. J. Sham. *Phys. Rev*., 1965, **140**, A1133.

39 (a) Casida, M. E. "Time-Dependent Density Functional Response Theory for Molecules". In Recent AdVances in Density Functional Methods; Chong, D. P., Ed.; World Scientific: Singapore, 1995; Vol. 1. (b) S. J. A. van Gisbergen, F. Kootstra, P. R. T. Schipper, O.V. Gritsenko, J. G. Snijders and E. J. Baerends, "Density-functional-theory response-property calculations with accurate exchange-correlation potentials", Phys. Rev. A **47**, 1998, 2556.

40 E. van Lenthe and E. J. Baerends. *J. Comput. Chem*. 2003, **24**, 1142.

41 C. Girardot, G. Lemercier, J.-C. Mulatier, J. Chauvin, P. L. Baldeck and C. Andraud, *Dalton Trans.* 2007, 3421-3426.

42 M. Abrahamsson, L. Hammarström, D. A. Tocher, S. Nag and D. Datta, *Inorg. Chem*. 2006, **45**, 9580.

43 N. Mataga, *Bull. Chem. Soc. Jpn*., 1963, **36**, 654; J. Guérin, C. Aronica, G. Boeuf, J. Chauvin, J. Moreau and G. Lemercier, *J. Lumin.* 2011, **131**, 2668.

44 G. Lemercier, M. Four and S. Chevreux, *Coord. Chem. Rev.*, 2018, **368**, 1.

45 (a) F. N. Castellano, H. Malak, I. Gryczynski and J. R. Lakowicz, *Inorg. Chem.* 1997, **36**, 5548; (b) S. K. Hurst, M. P. Cifuentes, J. P. L. Morrall, N. T. Lucas, I. R. Whittall, M. G. Humphrey, I. Asselberghs, A. Persoons, M. Samoc, B. Luther-Davies and A. C. Willis, *Organometallics.* 2001, **20**, 4664.

46 J. R. Lakowicz, F. N. Castellano, I. Gryczynski and Z. Gryczynski, J. D. Dattelbaum, *J. Photochem. Photobiol A*. 1999, **122**, 95.

47 C. E. Powell, J. P. Morrall, S. A. Ward, M. P. Cifuentes, E. G. A. Notars, M. Samoc and M. G. Humphrey, *J. Am. Chem. Soc*., 2004, **126**, 12234; J. L. Humphrey and D. Kuciauskas, *J. Am. Chem. Soc*., 2006, **128**, 3902.

48 (a) A. Colombo, C. Dragonetti, D. Roberto, A. Valore, C. Ferrante, I. Fortunati, A. L. Picone, F. Todescato and J. A. G. Williams, *Dalton Trans*., 2015, **44**, 15712; (b) E. M. Boreham, L. Jones, A. N. Swinburne, M. Blanchard-Desce, V. Hugues, C. Terryn, F. Miomandre, G. Lemercier and L. S. Natrajan, *Dalton Trans.*, 2015, **44**, 16127; (c) R. M. Edkins, S. L. Bettington, A. E. Goeta and A. Beeby, *Dalton Trans*., 2011, **40**, 12765 and references therein.

49 (a) S. W. Botchway, M. Charnley, J. W. Haycock, A. W. Parker, D. L. Rochester, J. A. Weinstein and J. A. G. Williams, *Proc. Natl. Acad. Sci. U. S. A*., 2008, **105**, 16071; (b) C. K. Koo, K.-L. Wong, C. W.-Y. Man, Y.-W. Lam, L. K.-Y. So, H.-L. Tam, S. W. Tsao, K.-W. Cheah, K.-C. Lau, Y.-Y. Yang, J.-C. Chen and M. H.-W. Lam, *Inorg. Chem*., 2009, **48**, 872.

50 (a) G.te Velde, F.M. Bickelhaupt, E.J. Baerends, C. Fonseca Guerra, S.J.A. van Gisbergen, J.G. Snijders and T. Ziegler, Chemistry with ADF, *J. Comput. Chem*., 2001, **22**, 931, DOI: 10.1002/jcc.1056. (b) C. Fonseca Guerra, J.G. Snijders, G. te Velde and E.J. Baerends. *Theor. Chem. Acc*., 1998, **99**, 391, DOI: 10.1007/s002140050353. (c) ADF2016, SCM, Theoretical Chemistry, Vrije Universiteit, Amsterdam, The Netherlands, http://www.scm.com. E.J. Baerends, T. Ziegler, A.J. Atkins, J. Autschbach, O. Baseggio, D. Bashford, A. Bérces, F.M. Bickelhaupt, C. Bo, P.M. Boerrigter, L. Cavallo, C. Daul, D.P. Chong, D.V. Chulhai, L. Deng, R.M. Dickson, J.M. Dieterich, D.E. Ellis, M. van Faassen, L. Fan, T.H. Fischer, C. Fonseca Guerra, M. Franchini, A. Ghysels, A. Giammona, S.J.A. van Gisbergen, A. Goez, A.W. Götz, J.A. Groeneveld, O.V. Gritsenko, M. Grüning, S. Gusarov, F.E. Harris, P. van den Hoek, Z. Hu, C.R. Jacob, H. Jacobsen, L.

Jensen, L. Joubert, J.W. Kaminski, G. van Kessel, C. König, F. Kootstra, A. Kovalenko, M.V. Krykunov, E. van Lenthe, D.A. McCormack, A. Michalak, M. Mitoraj, S.M. Morton, J. Neugebauer, V.P. Nicu, L. Noodleman, V.P. Osinga, S. Patchkovskii, M. Pavanello, C.A. Peeples, P.H.T. Philipsen, D. Post, C.C. Pye, H. Ramanantoanina, P. Ramos, W. Ravenek, J.I. Rodríguez, P. Ros, R. Rüger, P. R. T. Schipper, D. Schlüns, H. van Schoot, G. Schreckenbach, J.S. Seldenthuis, M. Seth, J.G. Snijders, M. Solà, M. Stener, M. Swart, D. Swerhone, V. Tognetti, G. te Velde, P. Vernooijs, L. Versluis, L. Visscher, O. Visser, F. Wang, T.A. Wesolowski, E. M. van Wezenbeek, G. Wiesenekker, S.K. Wolff, T. K. Woo and A. L. Yakovlev.

51 J. P. Perdew, K. Burke, M. *Phys. Rev. Lett*., 1996, **77**, 3865.

52 (a) O. V. Gritsenko, P. R.T. Schipper, E. J. Baerends. *Chem. Phys. Lett*., 1999, **302**, 199. (b) P.R.T. Schipper, O.V. Gritsenko, S. J. A. van Gisbergen and E. J. Baerends, *J. Chem. Phys*., 2000, **112**, 1344.

53 (a) E. van Lenthe, A. E. Ehlers and E. J. Baerends. *J. Chem. Phys*., 1999, **110**, 8943; (b) E. van Lenthe, E.J. Baerends and J. G. Snijders. *J. Chem. Phys*., 1994, **101**, 9783.